XLVI CILAMCE
VITÓRIA - ES - BRAZIL - 2025
XLVI IBERO-LATIN AMERICAN CONGRESS ON COMPUTATIONAL METHODS IN ENGENEERING

Simulation of procedures for water filling a sand experimental apparatus using a locally conservative two-phase formulation of the Finite Element Method

Giovane Avancini[1], Nathan Shauer[1], Gustavo H. Siqueira[1], Philippe R. B. Devloo[1]

[1]*Dept. de Estruturas, Universidade Estadual de Campinas (UNICAMP)*
Rua Saturnino de Brito, 224, Cidade Universitária Zeferino Vaz, Campinas - São Paulo, Brasil
giovanea@unicamp.br, shauer@unicamp.br, siqueira@fec.unicamp.br, phil@unicamp.br

Abstract. This work presents a locally conservative scheme to solve two-phase flow problems in heterogeneous porous media. The Darcy equations are discretized using a mixed formulation of the Finite Element Method (FEM) based on de Rham compatible spaces; i.e. $H(\text{div}, \Omega)$ functions to approximate the flux field and $L^2(\Omega)$ discontinuous functions for the pressure field. These choices ensure that mass conservation holds strongly and provide high order accuracy for the flux variables. For the transport problem, piecewise constant functions (Finite Volume Method) are used to approximate the saturation field. Quadratic relative permeability curves with residual saturation is adopted for both water and air, and a linear density function is considered to account for the air compressibility. The time-marching procedure is performed using a standard Backward-Euler method. The nonlinearity due to the coupling is solved using a Sequential Fully Implicit (FSI) strategy. The proposed scheme is applied to simulate an experiment on filling an initially unsaturated experimental apparatus using different water injection procedures.

Keywords: Multiphase flow, Local conservation, H(div) spaces, Compressible Darcy, Coupled problems

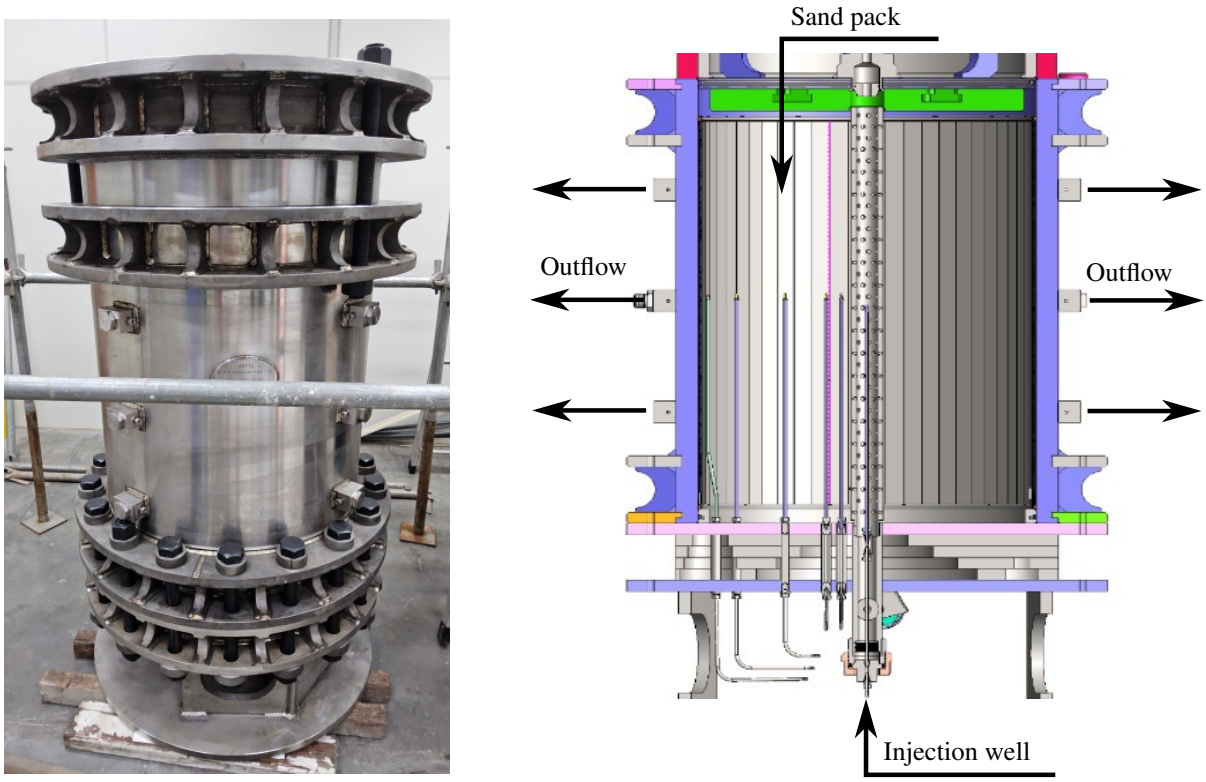
1 Introduction

A significant portion of oil extracted from mature wells is achieved through water injection techniques. However, changes in some reservoir properties–like permeability or porosity–can severely impair the formation, resulting in decreased well productivity [1]. Water injection processes are often associated with various formation damage mechanisms, including the migration of suspended solids, which may lead to pore blockage and the formation of a filter cake at the well-reservoir interface. Additionally, the mobilization of fine particles within the reservoir can further exacerbate flow impairment [2]. Thus, understanding the mechanisms of water injection and the resulting flow patterns is crucial for optimizing oil recovery processes.

At UNICAMP, an ongoing research project supported by TotalEnergies, the WIWIS (Wellbore Interface Well-scale Investigation System), is focused on experimentally investigating injectivity loss of produced water in reservoirs with the variation of physical and geometric parameters of the well. The core of the project involves the development of a realistic well simulator measuring 10 meters in length, composed of modular 1-meter segments that can be connected to replicate full-scale injection conditions (see Figure 1). This innovative apparatus is designed to enable a range of experimental tests, including linear and radial filtration, filter cake buildup, and other mechanisms associated with injectivity loss. Currently, the project is in its derisking phase, during which preliminary tests are being conducted using a single 1-meter module to validate the experimental setup and ensure the reliability of future large-scale tests.

Each module of the WIWIS apparatus consists of a 1000 mm long cylindrical casket with an external diameter of 670.95 mm and a central injection wellbore with a diameter of 64.8 mm. A sand screen is installed along the wellbore surface to prevent sand particle migration into the wellbore while allowing water to flow through. On the outer surface, a mesh diffuser is attached to promote uniform radial flow across the sand pack. The space between the sand screen and the mesh diffuser is filled with a carefully selected type of sand that mimics the properties of a real oil reservoir. Each module is instrumented with pressure sensors to measure the pressure drop across the sand pack and flow meters to monitor the water injection rate.

A major concern during the derisking phase is the proper sand pack preparation, which involves i) filling the apparatus with sand, ii) compacting the sand until a desired permeability is achieved, and iii) saturating the



(a) (b)

Figure 1. 1 meter module of the WIWIS experimental apparatus at UNICAMP. (a) Real picture and (b) cross-section schematic.

sand with water while avoiding the entrapment of air bubbles. The presence of air bubbles can lead to inaccurate measurements and compromise the validity of the experimental results. To address this challenge, different filling procedures must be tested to determine the most effective strategy to saturate the sandpack while diminishing the residual air left in the module. Numerical simulations can play a crucial role in this context by providing insights into the flow dynamics during the filling process.

In this context, we propose a numerical study to investigate the impact of different filling strategies on the saturation process using a two-phase flow formulation based on a locally conservative Mixed Finite Element Method (FEM). The scheme uses a Sequential Fully Implicit (SFI) approach to solve the coupled nonlinear equations arising from the Darcy and transport problems [3]. The Darcy problem includes both incompressible and compressible flow, and is solved in a mixed form using de Rham compatible spaces, ensuring strong mass conservation and high-order accuracy for the flux variables. The saturation transport problem is discretized using piecewise constant functions, and includes gravitational segregation effects.

2 Preliminary and notations

In this section, the mathematical problem for the two-phase flow of water and gas in porous media is presented. The following hypotheses are considered:

- The porous medium is rigid, i.e., the porosity and permeability are constant in time;
- There is no chemical reactions nor adsorption;
- The system is isothermal;
- Capillary effects are neglected;
- No mass transfer occurs between the phases;
- Viscosity is constant for both phases.

Let $\Omega \in \mathbb{R}^d$ be an open domain with boundary $\partial\Omega = \partial\Omega_D \cup \partial\Omega_N$, where $\partial\Omega_D$ and $\partial\Omega_N$ are the Dirichlet and Neumann boundaries, respectively, and $[0, T]$ is the time interval with $T > 0$. The governing equations are

written in a weighted pressure form according to [4]: find $\boldsymbol{u}, p, s_w$ such that:

$$(\mathcal{K}\lambda)^{-1}\boldsymbol{u} + \nabla p - G_\lambda = 0 \quad \text{in } \Omega \times [0,T], \tag{1a}$$

$$-\phi\frac{\partial}{\partial t}\left(\frac{s_\alpha}{b_\alpha}\right) - \nabla\cdot(\boldsymbol{u}) = 0 \quad \text{in } \Omega \times [0,T], \tag{1b}$$

$$\phi\frac{\partial}{\partial t}\left(\frac{s_w}{b_w}\right) - \nabla\cdot\left(f_w\boldsymbol{u} + f_w f_g \boldsymbol{u}_{G_{wg}}\right) = 0 \quad \text{in } \Omega \times [0,T], \tag{1c}$$

where $\alpha = w, g$ is the phase index (water and gas, respectively), ϕ is the porosity, $\mathcal{K}$ [m^2] the intrinsic permeability tensor (which for simplicity, is assumed to be isotropic), p [Pa] is the weighted pressure, s_α is the saturation of phase α, observing that $\sum_\alpha s_\alpha = 1$, b_α is the formation volume factor of phase α, defined as the ratio between the phase density at atmospheric conditions and at reservoir conditions, and $\boldsymbol{u} = \sum_\alpha \boldsymbol{u}_\alpha$ [m^3/m^{2}s] is the total volumetric flux. The variables λ, f_α, G_λ, and $\boldsymbol{u}_{G_{wg}}$ denote the fluid mobility, fractional flow, gravity force, and gravity flux, computed as follows:

$$\lambda = \sum_\alpha \lambda_\alpha, \quad \lambda_\alpha = \frac{k_{r\alpha}}{\mu_\alpha b_\alpha}, \quad \alpha = w, g,$$

$$f_\alpha = \frac{\lambda_\alpha}{\lambda}, \quad \alpha = w, g,$$

$$G_\lambda = \boldsymbol{g}\sum_\alpha f_\alpha \rho_\alpha,$$

$$\boldsymbol{u}_{G_{wg}} = \mathcal{K}\lambda\boldsymbol{g}(\rho_w - \rho_g).$$

In the above equations, μ_α and ρ_α are the viscosity and density of phase α, and the relative permeability $k_{r\alpha}$ is a function of the saturation s_α, which in this work, a quadratic relative permeability model with residual saturation $s_{\alpha,r}$ in the form

$$k_{r\alpha}(s_\alpha) = \begin{cases} 0, & s_\alpha < s_{\alpha,r}, \\ \left(\frac{s_\alpha - s_{\alpha,r}}{1 - s_{\alpha,r}}\right)^2, & s_{\alpha,r} \le s_\alpha < 1, \end{cases} \quad \alpha = w, g,$$

is adopted. The water is assumed to be incompressible, so $b_w = 1$, while the air density ρ_α is a function of the pressure p. Under small values of pressure, i.e. $p < 10$ atm, the air behaves as an ideal gas [5], so a linear density model can be used without significant loss of accuracy:

$$\rho_g(p) = \rho_{g,\text{ref}}(1 + c_g(p - p_{\text{ref}})), \tag{2}$$

where $\rho_{g,\text{ref}}$ is the reference density at pressure p_{ref}, and c_g is the compressibility modulus of the gas.

Equations (1a)-(1c) form a set of coupled equations where two subproblems can be identified: the Darcy problem in its mixed form, given by (1a)-(1b), and the water saturation transport problem (1c).

The boundary conditions for the Darcy subproblem are given by:

$$\boldsymbol{u}\cdot\boldsymbol{n} = \boldsymbol{u}_N \quad \text{on } \partial\Omega_N \times [0,T], \tag{3a}$$

$$p = p_D \quad \text{on } \partial\Omega_D \times [0,T], \tag{3b}$$

where $\boldsymbol{n}$ is the outward normal vector to the boundary, $\boldsymbol{u}_N$ is the prescribed flux on the Neumann boundary, and p_D is the prescribed pressure on the Dirichlet boundary. For the transport equation, the saturation is prescribed only on inlet boundaries:

$$s_w = s_{w_{in}} \quad \text{on } \partial\Omega_{in} \times [0,T], \tag{4}$$

given the initial condition

$$s_w(\boldsymbol{x}, t = 0) = s_w^0 \quad \text{in } \Omega. \tag{5}$$

3 Variational formulation and FEM discretization

The domain Ω is discretized using a finite element partition $\mathcal{T} = \{K_i : i = 1, ..., N\}$, where K is an element with usual shape. The Hilbert spaces $L^2(\Omega)$ and $H^1(\Omega)$ have their usual meaning and norms. The space $H(\text{div}, \Omega)$ comprises by vectorial functions $\boldsymbol{v} \in [L^2(\Omega)]^d$ whose divergence $\nabla\cdot\boldsymbol{v}$ belongs to $L^2(\Omega)$. The time is discretized

using a Backward-Euler scheme with uniform time steps Δt, so that $t^n = n\Delta t$, for $n = 0, 1, 2, ..., N_t$, where N_t is the total number of time steps. The superscript n indicates the value of a variable at time t^n.

For the Darcy subproblem, the following piece-wise functional spaces are considered:

$$\mathcal{V} = \{\boldsymbol{v} \in H(\text{div}, \Omega) : \boldsymbol{v} \cdot \boldsymbol{n} = \boldsymbol{u}_N \text{ on } \partial\Omega_N\},$$

$$\mathcal{P} \subset L^2(\Omega),$$

verifying the De Rham compatibility $\nabla \cdot \mathcal{V} \subset \mathcal{P}$ [6, 7]. For the transport subproblem, the space $\bar{\mathcal{P}}$ of piece-wise constant functions over $\mathcal{T}$, yielding a finite volume formulation.

The weak form of Eqs. (1a)-(1c) then reads: find $(\boldsymbol{u}, p, s_w) \in (\mathcal{V}, \mathcal{P}, \bar{\mathcal{P}})$ such that:

$$((\mathcal{K}\lambda^{n+1})^{-1}\boldsymbol{u}^{n+1}, \boldsymbol{v})_{\mathcal{T}} - (p^{n+1}, \nabla \cdot \boldsymbol{v})_{\mathcal{T}} = (G_\lambda^{n+1}, \boldsymbol{v})_{\mathcal{T}} - \langle p_D, \boldsymbol{v} \cdot \boldsymbol{n}\rangle_{\partial\Omega_D}, \quad \forall \boldsymbol{v} \in \mathcal{V}_0, \tag{6a}$$

$$-(\nabla \cdot \boldsymbol{u}, q)_{\mathcal{T}} - (\frac{\phi}{\Delta t}\frac{s_\alpha^{n+1}}{b_\alpha^{n+1}}, q)_{\mathcal{T}} = -(\frac{\phi}{\Delta t}\frac{s_\alpha^{n}}{b_\alpha^{n}}, q)_{\mathcal{T}}, \quad \forall q \in \mathcal{P}, \tag{6b}$$

$$(\phi s_w^{n+1}, d)_{\mathcal{T}} + \langle \Delta t \mathcal{F}^{n+1}, d\rangle_{\partial\mathcal{T}\setminus\partial\Omega_{in}} = (\phi s_w^n b_w^n, d)_{\mathcal{T}} - \langle \Delta t s_{w_{in}} \boldsymbol{u}^{n+1} \cdot \boldsymbol{n}, d\rangle_{\partial\Omega_{in}}, \quad \forall d \in \bar{\mathcal{P}}, \tag{6c}$$

where

$$\mathcal{F}^{n+1} = \mathcal{F}(s_w^{n+1}, \boldsymbol{u}^{n+1}) = f_w(s_w^{n+1})\boldsymbol{u}^{n+1} + f_w(s_w^{n+1})f_g(s_w^{n+1})\boldsymbol{u}_{G_{wg}}^{n+1}$$

is a nonlinear function if the gravitational flux $\boldsymbol{u}_{G_{wg}}$ is not null. To solve problem (6c), the Implicit Hybrid Upwinding (IHU) [8] method is used. The tangent matrix can be obtained by differentiating Eqs. (6a)-(6c) with respect to the unknowns $(\boldsymbol{u}, p, s_w)$, where a Newton's like method is used to iteratively solve them.

4 Sequential Fully Implicit (SFI) scheme

The coupled nonlinear equations (6a)-(6c) are solved using a Sequential Fully Implicit (SFI) scheme, which consists on splitting the system into two subproblems: the Darcy problem (6a)-(6b) and the transport problem (6c). The SFI scheme is summarized in Algorithm 1.

Algorithm 1: SFI algorithm

Input: $(\boldsymbol{u}, p, s_w)^n$, m_{sfi}, ε_p, ε_s
Output: $(\boldsymbol{u}, p, s_w)^{n+1}$ for a time step increment Δt

Set $m \leftarrow 1$;
Set $(\tilde{\boldsymbol{u}}, \tilde{p}, \tilde{s}_w)^m \leftarrow (\boldsymbol{u}, p, s_w)^n$;
for $m \in \{1, \ldots, m_{sfi}\}$ **do**
    (1) Update $\lambda(\tilde{s}_w^m)$;
    (2) Solve Eqs. (6a)-(6b) to obtain $(\tilde{\boldsymbol{u}}, \tilde{p})^{m+1}$;
    (3) Transfer $\tilde{\boldsymbol{u}}^{m+1}$ to transport solver and update ρ_g^{n+1} through Eq. (2);
    (4) Solve Eq. (6c) to obtain $\tilde{s}_w^{m+1}$;
    if $\left\|p^{m+1} - p^m\right\| \leq \varepsilon_p$ ***and*** $\left\|s_w^{m+1} - s_w^m\right\| \leq \varepsilon_s$ **then**
        Stop SFI iteration;
        Set $(\boldsymbol{u}, p, s_w)^{n+1} \leftarrow (\tilde{\boldsymbol{u}}, \tilde{p}, \tilde{s}_w)^{m+1}$;
        return $(\boldsymbol{u}, p, s_w)^{n+1}$;

5 Numerical results

In this section, the proposed numerical scheme is applied to simulate the filling of the WIWIS experimental apparatus using different water injection procedures. The module is represented by a 2D axisymmetric domain as shown in Figure 2. The sand pack is initially full with air ($s_w^0 = 0$), and water is injected through the central wellbore at a constant flow rate $Q_w = 5$ L/min, so the water height in the wellbore increases over time by the expression:

$$h_w(t)^{n+1} = h_w(t)^n + \frac{(Q_w - Q_{in}^n)\Delta t}{\pi r_w^2},$$

where Q_{in} is the injected rate in the porous media and $r_w = 0.0324$ m is the wellbore radius. No-flow conditions are imposed at the outer surface (as during the filling the valves are closed), base, and lid (except for a small gap

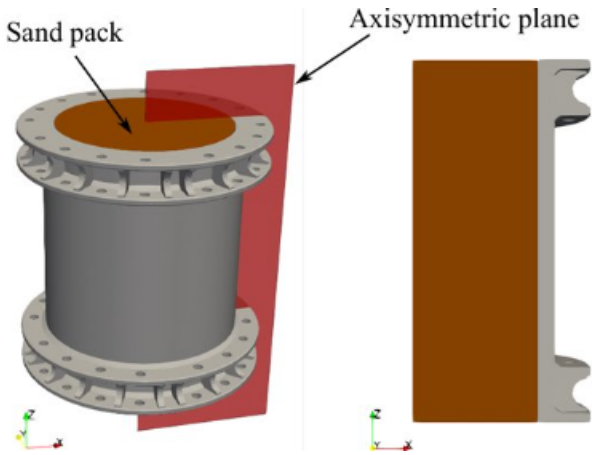


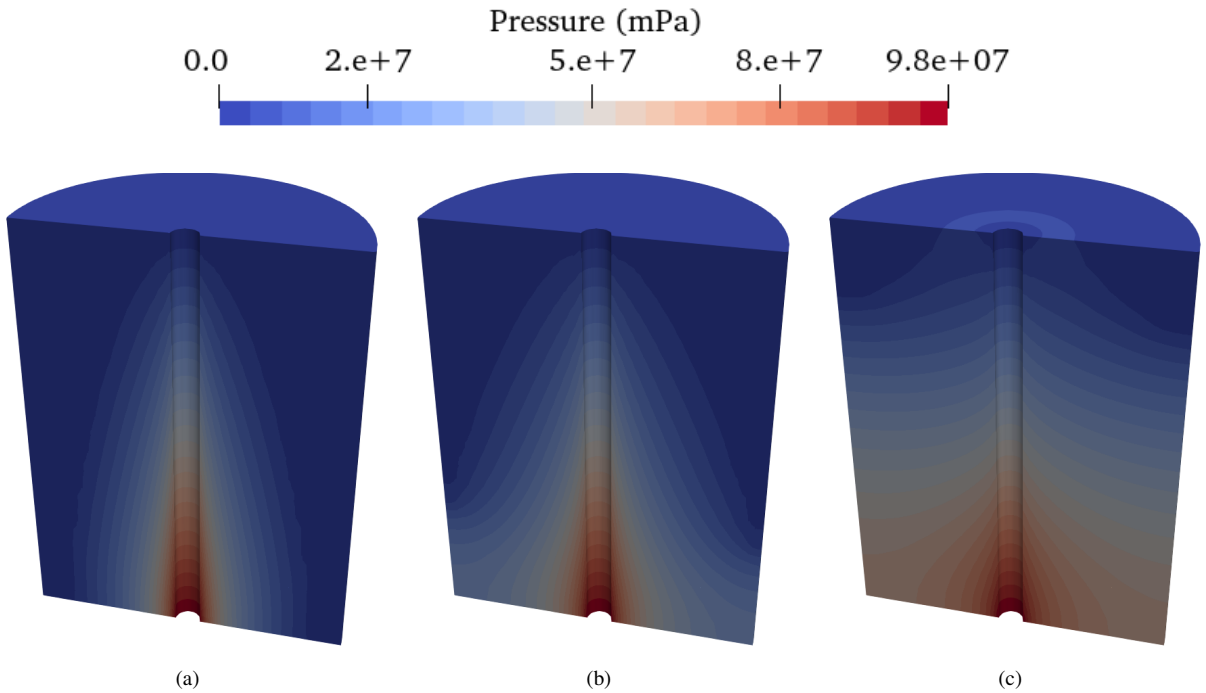
Figure 2. 1-meter module represented by a 2D axisymmetric domain.

Table 1. Physical properties used in the simulations.

Property	Value
Porosity (ϕ)	0.35
Permeability ($\mathcal{K}$)	500 mD
Water viscosity (μ_w)	1.0×10^{-3} Pa·s
Air viscosity (μ_g)	1.8×10^{-5} Pa·s
Water density (ρ_w)	1000 kg/m^3
Air density ($\rho_{g,\text{ref}}$)	1.2 kg/m^3
Air compressibility (c_g)	1.0×10^{-5} Pa^{-1}
Residual water saturation ($s_{w,r}$)	0.2
Residual air saturation ($s_{g,r}$)	0.2

at the top close to the outer surface that acts as a purge vent). The physical properties of the sand and fluids used in the simulations are summarized in Table 1.

The numerical simulation is performed using a uniform mesh with 400 elements, and the time step is set to $\Delta t = 0.025$ s. The SFI algorithm is executed with $m_{sfi} = 5$ iterations and convergence tolerances $\varepsilon_p = \varepsilon_s = 10^{-6}$. Figure 3 shows the pressure distribution of the reservoir at different times during the filling process, while Figure 4 depicts the water saturation evolution. The results indicate that the water front moves almost radially outward from the wellbore, gradually saturating the sand pack from the bottom to the top. The pressure increases as the water fills the voids, and the saturation reaches a maximum value of approximately 0.8, as expected due to the residual air saturation considered in the relative permeability model.

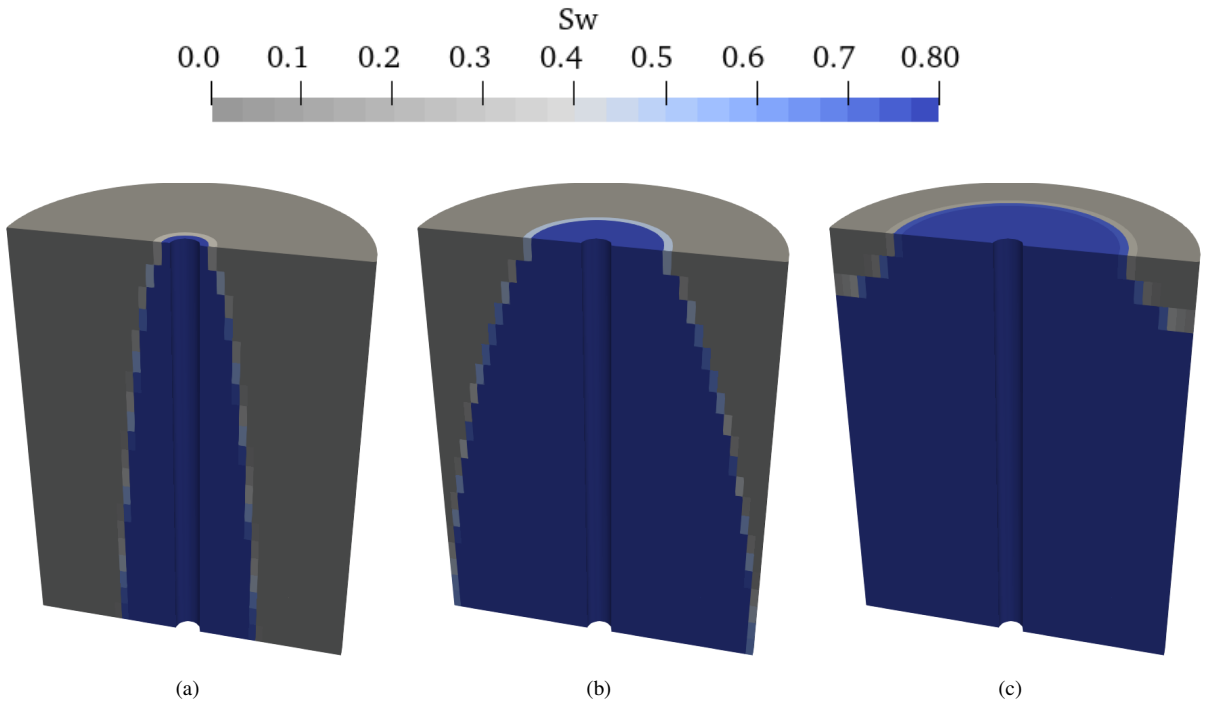


(a) (b) (c)

Figure 3. Pressure distribution in the sand pack after (a) $t = 500$ s, (b) $t = 1000$ s, and (c) $t = 1500$ s.

6 Conclusions

This work presented a locally conservative mixed finite element scheme for simulating two-phase flow in heterogeneous porous media, with application to the filling process of a sand experimental apparatus. The math-



(a) (b) (c)

Figure 4. Water saturation after (a) $t = 100$ s, (b) $t = 800$ s, and (c) $t = 1700$ s.

ematical model incorporates compressible air and incompressible water, and is solved using a Sequential Fully Implicit (SFI) strategy that efficiently handles the nonlinear coupling between flow and transport. The numerical results demonstrate the capability of the proposed approach to capture the evolution of pressure and saturation fronts during water injection, providing valuable insights into the dynamics of sandpack saturation and the mitigation of air entrapment. Future work may extend the methodology to include additional physical effects, such as capillarity, and to explore more complex injection scenarios by applying vacuum at the purge vent to enhance air removal.

Acknowledgements. We gratefully acknowledge the support of Total Energies Brazil through FUNCAMP (Process 76042-23) and the Brazilian National Council for Scientific and Technological Development (grants 305823/2017-5 and 309597/2021-8). We also acknowledge the support of ANP (Brazil's National Oil, Natural Gas and Biofuels Agency).

Authorship statement. The authors hereby confirm that they are the sole liable persons responsible for the authorship of this work, and that all material that has been herein included as part of the present paper is either the property (and authorship) of the authors, or has the permission of the owners to be included here.

References

[1] C. Esene, N. Rezaei, A. Aborig, and S. Zendehboudi. Comprehensive review of carbonated water injection for enhanced oil recovery. *Fuel*, vol. 237, pp. 1086–1107, 2019.
[2] D. Bennion, D. Bennion, F. Thomas, and R. Bietz. Injection water quality-a key factor to successful waterflooding. *Journal of Canadian Petroleum Technology*, vol. 37, n. 06, 1998.
[3] O. Duran, P. R. Devloo, S. M. Gomes, and J. Villegas. A multiscale mixed finite element method applied to the simulation of two-phase flows. *Computer Methods in Applied Mechanics and Engineering*, vol. 383, pp. 113870, 2021.
[4] Z. Chen. Formulations and numerical methods of the black oil model in porous media. *SIAM Journal on Numerical Analysis*, vol. 38, n. 2, pp. 489–514, 2000.
[5] Y. A. Cengel and M. A. Boles. Thermodynamics: an engineering approach. *Sea*, vol. 1000, n. 8862, pp. 287–93, 2002.
[6] D. De Siqueira, P. R. Devloo, and S. M. Gomes. A new procedure for the construction of hierarchical high order hdiv and hcurl finite element spaces. *Journal of Computational and Applied Mathematics*, vol. 240, pp.

204–214, 2013.

[7] P. R. Devloo, J. W. Fernandes, S. M. Gomes, F. T. Orlandini, and N. Shauer. An efficient construction of divergence-free spaces in the context of exact finite element de rham sequences. *Computer Methods in Applied Mechanics and Engineering*, vol. 402, pp. 115476, 2022.

[8] J. Jiang and H. A. Tchelepi. Nonlinear acceleration of sequential fully implicit (sfi) method for coupled flow and transport in porous media. *Computer Methods in Applied Mechanics and Engineering*, vol. 352, pp. 246–275, 2019.